GROWING MODES OF THE FREE-ELECTRON LASER AND THEIR BANDWIDTH*

G. Wang#, V. N. Litvinenko, BNL, Upton, NY 11973, U.S.A.
S. D. Webb, Tech-X Corporation, Boulder, CO 80303, U.S.A.

Abstract

We studied in detail the FEL dispersion relation for a spatially uniform electron beam, taking into account energy spread and the effects of space charge. We derived the maximum number of growing modes and the upper frequency cut-off for energy distributions satisfying a few constraints. Since the FEL dispersion relation for an infinite electron beam can be reduced to the 1D FEL dispersion relations when the radiation propagates along the undulation's axis, our analyses and findings directly are applicable to 1D FELs.

INTRODUCTION

We previously introduced a method of determining the number of growing modes and calculating their high frequency cut-off for the 1D FEL dispersion relation in the absence of the space- charge effects [1]. By allowing the radiation fields to propagate at an angle with respect to the undulator's axis, while assuming that the electrons move along constrained helical trajectories parallel with the undulator's axis, we were able to derive a dispersion relationship for a spatially uniform electron beam [2]; furthermore, it is reducible to the 1D FEL dispersion relation provided that the radiation propagates along the undulator's axis.

In this work, we started with the FEL dispersion relation we derived earlier [2] for a spatially uniform electron-beam, and investigated the number of growing modes and their high frequency cut-off , taking into account the space-charge effects. In section II, for an unspecified energy distribution satisfying certain constraints, we derive the formula for determining the maximal number of growing modes and their high frequency cut-off. Section III contains some examples where we apply the formula to several frequently encountered energy distributions and compare our results with direct numerical solutions of the dispersion relations. We summarize our findings in Section IV.

MAXIMAL NUMBER OF GROWING MODES

Assuming that electrons have a uniform spatial distribution and move along helical trajectories in parallel with the undulator's axis, the FEL dispersion relation is [2]

$$s = \left(1 + is\hat{\Lambda}_p^2\right)D(s), \tag{1}$$

where s is the Laplace transformation-variable of the normalized longitudinal location $\hat{z} \equiv \Gamma z$,

$$\hat{\Lambda}_p \equiv \frac{1}{\Gamma}\left[\frac{4\pi j_0}{\gamma_z^2 \gamma I_A}\right]^{1/2}$$

is the space-charge parameter,

$$\Gamma \equiv \left[\frac{\pi j_0 \theta_s^2 \omega}{c\gamma_z^2 \gamma I_A}\right]^{1/3},$$

is the 1D FEL gain parameter, $I_A \equiv m_e c^3/e$ is the Alfven current, ω is the radiation frequency, v_z is the longitudinal velocity of electrons, γ_z is the Lorentz parameter for v_z, and $\hat{\Delta}_{3d} \equiv \hat{\Delta} + \hat{k}_\perp^2$ is the normalized detuning parameter defined for the radiation field propagating with a transverse angle,

$$\hat{\Delta} \equiv -\frac{1}{\Gamma}\left[k_w + \frac{\omega}{c} - \frac{\omega}{v_z}\right]$$

is the normalized detuning parameter, $k_w = 2\pi/\lambda_w$ is the undulator's wave number, $\rho = \gamma_z^2 \Gamma c/\omega$ is the Pierce parameter, and the normalized transverse wave-vector is defined as

$$\hat{\vec{k}}_\perp \equiv \sqrt{\frac{\rho}{2}}\frac{\vec{k}_\perp}{\gamma_z \Gamma}.$$

The dispersion integral in eq. (1) is defined as

$$D(s) \equiv \int_{-\infty}^{\infty} d\hat{P} \frac{d\hat{F}(\hat{P})}{d\hat{P}} \frac{1}{s + i\left(\hat{P} - \hat{\Delta}_{3d}\right)}, \tag{2}$$

for any root of eq. (1) with $\mathrm{Re}(s) > 0$ to correspond to an exponential growing FEL instability. To explore the roots of eq. (1) with $\mathrm{Re}(s) > 0$, we define a complex function

$$w(s) \equiv s - is\hat{\Lambda}_p^2 D(s) - D(s) \tag{3}$$

and consider a mapping from the complex s plane to the complex $w(s)$ plane along the contour $\mathcal{C}$, which comprises a vertical straight line parallel to the imaginary axis, $\mathcal{C}_1$, and a semi-circle in the right half complex plane, $\mathcal{C}_2$, as illustrated in fig. 1 (a). Fig. 1 (b) shows the map of $\mathcal{C}$ in the complex $w(s)$ plane, $\mathcal{D}$, with $\mathcal{D}_1$ and $\mathcal{D}_2$ being, respectively, the map of $\mathcal{C}_1$ and $\mathcal{C}_2$. For an energy distribution $\hat{F}(\hat{P})$ falling faster than Lorentzian distribution, we previously proved that the map from $\mathcal{C}_2$ to $\mathcal{D}_2$ has the asymptotic property

$$\lim_{|s|\to\infty}\left|\hat{D}(s)\right| \le \sqrt{2}\pi\hat{q}\hat{F}_{\max} \lim_{|s|\to\infty}\frac{1}{|s|^2}\left[1 + \frac{\hat{q}}{\mathrm{Re}(s)}\right], \tag{4}$$

* Work supported by Brookhaven Science Associates, LLC under Contract No.DE-AC02-98CH10886 with the U.S. Department of Energy.
#gawang@bnl.gov

ISBN 978-3-95450-123-6

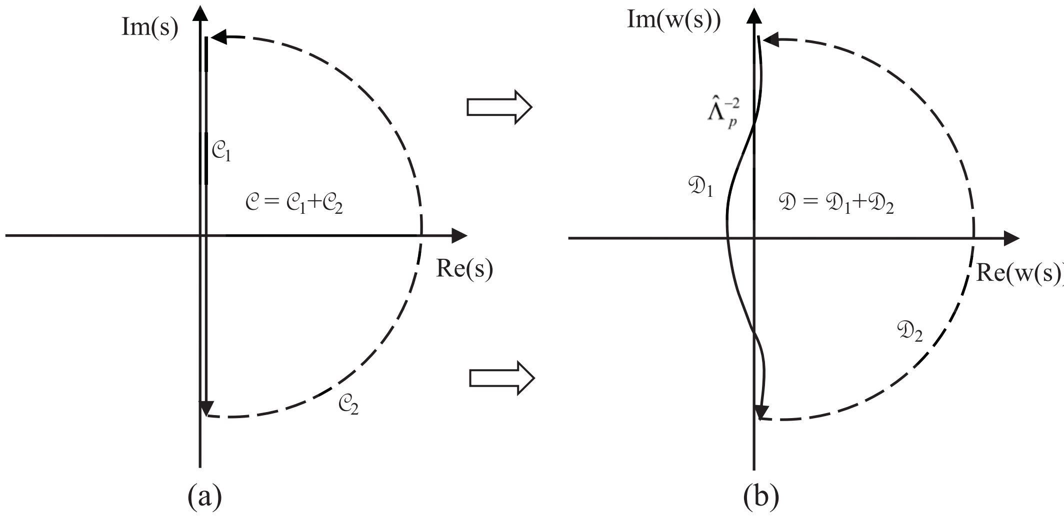

Figure 1: Mapping from s to w(s) as defined in eq. (3). We assumed that the energy distribution satisfies eq. (5); hence, the map from $\mathcal{C}_2$ to $\mathcal{D}_2$ approaches an identity map as |s| nears infinity as shown in eq. (6).

where $\hat{F}_{\max}$ is the maximum of $\hat{F}(\hat{P})$ and $\hat{q}$ is a positive number that satisfies,

$$\hat{F}(\hat{P})\leq\frac{\hat{F}_{\max}}{1+\hat{P}^2/\hat{q}^2}\ ,\ \forall\hat{P}. \qquad (5)$$

Applying eq. (4) to eq. (3) leads to*

$$\lim_{|s|\to\infty}\left|\left(1+is\hat{\Lambda}_p^2\right)D(s)\right|\leq\lim_{|s|\to\infty}\left|D(s)\right|+\hat{\Lambda}_p^2\lim_{|s|\to\infty}|s|\left|D(s)\right|=0\ , \qquad (6)$$

suggesting that the map from $\mathcal{C}_2$ to $\mathcal{D}_2$ asymptotically approaches an identity map as the radius of $\mathcal{C}_2$ moves towards infinity. Assuming $\mathcal{C}_1$ is infinitely close to the imaginary axis leads to

$$s=\varepsilon_+ + it\ , \qquad (7)$$

where ε_+ is an infinitesimal positive number, and t is a real number going from ∞ to $-\infty$ along $\mathcal{C}_1$. Inserting eq. (7) into eq. (2) and taking the limit $\varepsilon_+\to 0$ yields

$$D(it)=\pi\left.\frac{d\hat{F}(\hat{P})}{d\hat{P}}\right|_{\hat{P}=\hat{\Delta}_{3d}-t}-iP.V.\int_{-\infty}^{\infty}d\hat{P}\frac{d\hat{F}(\hat{P})}{d\hat{P}}\frac{1}{t-\hat{\Delta}_{3d}+\hat{P}}\ . \qquad (8)$$

Hence, the map from $\mathcal{C}_1$ to $\mathcal{D}_1$ as calculated from eq. (3) reads

$$w(it)=i\left[t+\left(1-t\hat{\Lambda}_p^2\right)P.V.\int_{-\infty}^{\infty}d\hat{P}\frac{d\hat{F}(\hat{P})}{d\hat{P}}\frac{1}{t-\hat{\Delta}_{3d}+\hat{P}}\right]-\left(1-t\hat{\Lambda}_p^2\right)\pi\left.\frac{d\hat{F}(\hat{P})}{d\hat{P}}\right|_{\hat{P}=\hat{\Delta}_{3d}-t}. \qquad (9)$$

As t monotonically decreases from ∞ to $-\infty$, $\mathcal{D}_1$ intersects with the imaginary axis at

$$t=t_0=\hat{\Lambda}_p^{-2}\ , \qquad (10)$$

with the intersecting point at the imaginary axis of the $w(s)$ plane given by

$$w(it)=i\hat{\Lambda}_p^{-2}\ , \qquad (11)$$

and

$$t=t_n \quad \text{for} \quad n=1,2,\ldots N_{le}\ , \qquad (12)$$

where N_{le} is the total number of local extremas of $\hat{F}(\hat{P})$ and t_n as determined by the condition†

$$\left.\frac{d\hat{F}(\hat{P})}{d\hat{P}}\right|_{\hat{P}=\hat{\Delta}_{3d}-t_n}=0\quad . \qquad (13)$$

If $D(s)$ is meromorphic in the $\mathrm{Re}(s)>0$ half plane and has no poles or zeros along $\mathcal{C}$, from the principle of this argument, the number of solutions of the dispersion relation, eq. (1), is given by

$$Z=W+P\ , \qquad (14)$$

wherein P is the number of poles of function $w(s)$ enclosed by the contour, $\mathcal{C}$, in the complex s plane (fig.2b), and W is the winding number of $\mathcal{D}$ around the origin of the complex $w(s)$ plane. In addition, the derivative of $D(s)$ for $\mathrm{Re}(s)>0$ satisfies the following

* In the case where $\mathrm{Re}(s)$ is approaching zero, we always can ensure that the imaginary of s grows faster than $\mathrm{Re}(s)^{-1}$ such that $|s|\geq\mathrm{Im}(s)=\mathrm{Re}(s)^{-2}$, and hence eq. (6) is satisfied.

† In cases where $\hat{F}(\hat{P})$ is smooth and any order of its derivative is continuous, t_n always are discrete numbers. If $\hat{F}(\hat{P})$ is not smooth, there might be some continuous range of t wherein eq. (13) is satisfied. In that case, each continuous range is counted as one intersection in eq. (12) .

ISBN 978-3-95450-123-6

$$\left|\frac{d}{ds}D(s)\right| = \left|\int_{-\infty}^{\infty} d\hat{P}\frac{d\hat{F}(\hat{P})}{d\hat{P}}\frac{1}{\left[s+i\left(\hat{P}-\hat{\Delta}_{3d}\right)\right]^2}\right| \le \frac{1}{\mathrm{Re}(s)^2}\int_{-\infty}^{\infty} d\hat{P}\left|\frac{d\hat{F}(\hat{P})}{d\hat{P}}\right| \quad (15)$$

and hence, as long as $\int_{-\infty}^{\infty}\left|\frac{d}{d\hat{P}}\hat{F}(\hat{P})\right|d\hat{P}$ is bounded, $D(s)$ always is analytic in the right half plane, thus leading to[‡]

$$Z = W \quad (16)$$

i.e., the number of growing modes corresponds to the winding number. Eqs. (10) and (12) suggest that as t monotonically decreases from ∞ to $-\infty$, $\mathfrak{D}$ intersects with the imaginary axis for $N_{le}+1$ times. For a realistic distribution- function with the constraints

$$\lim_{\hat{P}\to\pm\infty}\hat{F}(\hat{P}) = 0 ,$$

N_{le} always is odd and equal to $2M-1$, where M is number of maxima of the energy distribution function. For each increases of winding number, the contour has to intersect with the imaginary axis twice and consequently, the maximal number of growing modes is equal to[§]

$$Z_{\max} = \frac{N_{le}+1}{2} = M , \quad (17)$$

i.e. the number of maxima of the energy distribution function. As eq. (9) implies, for given energy distribution and space-charge parameter, contour $\mathfrak{D}_1$ solely depends on the detuning parameter $\hat{\Delta}_{3d}$. As we see later, by investigating where $\mathfrak{D}_1$ intersects the imaginary axis, we can determine the frequency regions for FEL instability.

EXAMPLES FOR ENERGY DISTRIBUTION HAVING ONE EXTREMUM

Assuming $\hat{F}(\hat{P})$ has only a local maximum at $\hat{P}=0$ and satisfies the constraints described in previous sections, eq. (17) suggests that, at most, there is one growing mode. As shown in fig. 2, $\mathfrak{D}_1$ intersects twice with the imaginary axis . One of the intersections happens at

$$t = \hat{\Lambda}_p^{-2}$$

and, according to eq. (13), the other intersection occurs at

$$t_1 = \hat{\Delta}_{3d} \quad (18)$$

with the intersecting point in the $w(s)$ plane given by

$$w(it_1) = i\left[\hat{\Delta}_{3d} + \left(1-\hat{\Delta}_{3d}\hat{\Lambda}_p^2\right)P.V.\int_{-\infty}^{\infty} d\hat{P}\frac{d\hat{F}(\hat{P})}{d\hat{P}}\frac{1}{\hat{P}}\right]. \quad (19)$$

Since at $t=-\infty$,

$$\mathrm{Re}\left[w(-i\infty)\right] = -\lim_{T\to\infty}\left(1+T\hat{\Lambda}_p^2\right)\pi\left.\frac{d\hat{F}(\hat{P})}{d\hat{P}}\right|_{\hat{P}=T+\hat{\Delta}_{3d}} > 0 \quad (20)$$

and, at $t=\infty$

$$\mathrm{Re}\left[w(i\infty)\right] = -\lim_{T\to\infty}\left(1-T\hat{\Lambda}_p^2\right)\pi\left.\frac{d\hat{F}(\hat{P})}{d\hat{P}}\right|_{\hat{P}=\hat{\Delta}_{3d}-T}, \quad (21)$$

$$= \lim_{T\to\infty}T\hat{\Lambda}_p^2\pi\left.\frac{d\hat{F}(\hat{P})}{d\hat{P}}\right|_{\hat{P}=\hat{\Delta}_{3d}-T} > 0$$

depending on the value of eq. (19), $\mathfrak{D}_1$ behaves as one of the three scenarios shown in fig. 2. If $\mathfrak{D}_1$ crosses the origin of the $w(s)$ plane as shown in fig . 2(b), eq. (19) vanishes, leaving the cut-off detuning parameter as[**]

$$\hat{\Delta}_{3d}^{+} = -\frac{P.V.\int_{-\infty}^{\infty} d\hat{P}\frac{d\hat{F}(\hat{P})}{d\hat{P}}\frac{1}{\hat{P}}}{1-\hat{\Lambda}_p^2 P.V.\int_{-\infty}^{\infty} d\hat{P}\frac{d\hat{F}(\hat{P})}{d\hat{P}}\frac{1}{\hat{P}}}. \quad (22)$$

Table 1 lists the expressions for the cut-off detuning parameters as we calculated from eq. (22) for some frequently used energy distributions. The general dependence of high frequency cut-off on the energy spread and space-charge parameter has the form $\hat{\Delta}_{3d}^{+} = \left(a\cdot\sigma^2+\hat{\Lambda}_p^2\right)^{-1}$, with the coefficient a determined by the specific form of the energy distribution. Inserting Gaussian distribution as shown in Table 1 into eq. (9) yields

$$w(it) = -\left(1-t\hat{\Lambda}_p^2\right)\pi\left.\frac{d\hat{F}(\hat{P})}{d\hat{P}}\right|_{\hat{P}=\hat{\Delta}_{3d}-t} + i\left\{t-\frac{1-t\hat{\Lambda}_p^2}{\sigma^2}\times\left[1-\sqrt{\pi}\cdot\left(\frac{\hat{\Delta}_{3d}-t}{\sqrt{2}\sigma}\right)\cdot Erfi\left(\frac{\hat{\Delta}_{3d}-t}{\sqrt{2}\sigma}\right)\cdot e^{-\frac{(\hat{\Delta}_{3d}-t)^2}{2\sigma^2}}\right]\right\}. \quad (23)$$

Fig.2 shows how contour $\mathfrak{D}_1$ changes with detuning, implying that the winding number, and hence, the number of growing modes change from 1 to 0 as the detuning rises above 0.8. Fig. 3 shows the numerical solution of the dispersion relation, eq. (1), with the dispersion integral given by [3]

$$D(s) = \frac{i}{\hat{\sigma}^2} - \frac{i\sqrt{\pi/2}}{\hat{\sigma}^3}\left(s-i\hat{\Delta}\right)\exp\left[\frac{\left(s-i\hat{\Delta}\right)^2}{2\hat{\sigma}^2}\right]\cdot\left[1-Erf\left(\frac{s-i\hat{\Delta}}{\sqrt{2}\hat{\sigma}}\right)\right] \quad (24)$$

in agreement with the conclusion in eq. (17) and Table 1 on the number of growing modes and the cut-off frequency.

[‡] As the contour $\mathfrak{C}$ remains in the right half plane where $w(s)$ is analytic, there is no pole along $\mathfrak{C}$. However, possibly there are zeros along $\mathfrak{C}_1$ that correspond to a purely imaginary root and hence, do not entail an increase of the growing root.

[§] We note that N_{le} cannot be zero as required by our assumption in eq. (5).

[**] In the case where $\hat{F}(\hat{P})$ solely depends on $\hat{P}^2$, typically there are no singularities in the integrand, and hence, the principal value of the integration need not be taken.

ISBN 978-3-95450-123-6

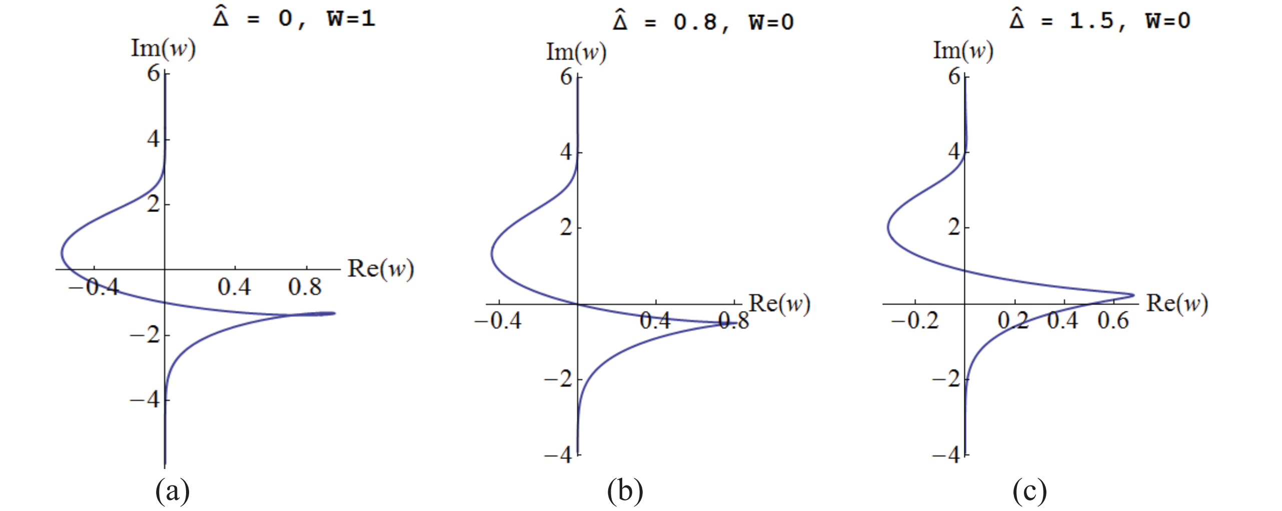

Figure 2: Mapping from s to w(s) as defined in eq. (3). We assume the energy distribution satisfies eq. (5), and hence, the map from $\mathcal{C}_s$ to $\mathcal{D}_s$ approaches an identity map as |s| approaches infinity as shown in the eq.(6).

Table 1: Cut-off Frequency of FEL

	Distribution function	$\hat{\Delta}^{+}_{3d}$
κ-n	$F(x)=\frac{\Gamma(n)}{\sqrt{n}\Gamma(n-1/2)} \times \frac{1}{\sqrt{2\pi}\sigma\left(1+\frac{x^2}{2n\sigma^2}\right)^n}$	$\frac{1}{\frac{2n}{2n-1}\sigma^2+\hat{\Lambda}_p^2}$
Gaussian	$F(x)=\frac{1}{\sqrt{2\pi}\sigma}e^{-\frac{x^2}{2\sigma^2}}$	$\frac{1}{\sigma^2+\hat{\Lambda}_p^2}$

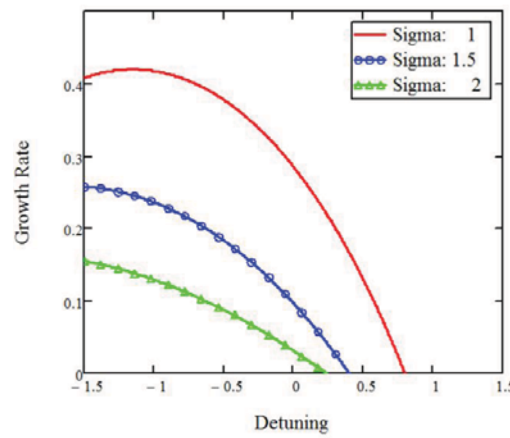

Figure 3: Numerical solution of the FEL growth rate for a Gaussian energy-distribution with various energy-spreads and $\hat{\Lambda}_p = 0.5$.

SUMMARY

In this work, we show that provided that the energy distribution of the electron beam, $\hat{F}(\hat{P})$, satisfies the following conditions:

- $\hat{F}(\hat{P})$ is differentiable for real $\hat{P}$;
- there exists a positive number M, such that
$$\int_{-\infty}^{\infty}\left|\frac{d}{d\hat{P}}\hat{F}(\hat{P})\right|d\hat{P}\le M;$$
- hence, there exists two positive numbers, $\hat{F}_{\max}$ and $\hat{q}$, such that
$$\hat{F}(\hat{P})\le\frac{\hat{F}_{\max}}{1+\hat{P}^2/\hat{q}^2},\ \forall\hat{P},$$

the maximal number of growing modes for a FEL with spatially uniform electron beam does not exceed the number of maxima of the energy distribution function. In addition, if $\hat{F}(\hat{P})$ has only one local maximum at $\hat{P}=0$, then the high frequency cut-off is determined by eq. (22). These results directly are applicable to the 1D FEL model by setting the transverse wave vector, $\vec{k}_\perp$, to zero. As our analyses are based on a dispersion relation derived for a spatially uniform electron beam, it certainly is not applicable when effects due to background electron density variation become important and the dispersion relation explored here does not hold anymore.

REFERENCES

[1] S. Webb, V. N. Litvinenko, and G. Wang, Physical Review Special Topic- Accelerator and Beam **15** (2012).
[2] S. Webb, G. Wang, and V. Litvinenko, Physical Review Special Topics - Accelerators and Beams **14** (2011).
[3] E. L. Saldin, E. A. Schneidmiller, and M. V. Yurkov, *The Physics of Free Electron Lasers* (Springer, New York, 1999).

ISBN 978-3-95450-123-6